International Journal of QUANTUM CHEMISTRY

Evaluation of the Molecular Static and Dynamic First Hyperpolarizabilities

Marc de Wergifosse, Vincent Liégeois, and Benoît Champagne*

By considering two prototypical π-conjugated compounds, several technical aspects associated with the evaluation of the first hyperpolarizabilities have been addressed in this article, that is, (i) the automatization of the Romberg's scheme to improve the numerical accuracy in the finite field method, (ii) the evaluation of the frequency dispersion at correlated levels using approximate schemes, and (iii) the deviations from Kleinman's symmetry conditions. It results from this study that accurate numerical derivatives can be obtained by resorting to the Romberg's method and by analyzing the Romberg's table in terms of two quantities, the field error and the iteration error. Indeed, the resulting first hyperpolarizability values are in close agreement with those obtained using an analytical differentiation procedure. The reliability of the multiplicative and additive approximate schemes to describe the frequency dispersion at correlated levels from using HF (Hartree-Fock) frequency dispersion has been confirmed to be limited to large wavelengths or far-from-resonance wavelength regions. Kleinman's symmetry conditions have been assessed, showing that for off-diagonal components of these two π-conjugated compounds, the deviations could be substantial. Nevertheless, good accuracy can be achieved for experimentally related quantities like β_{HRS} because the diagonal tensor components are dominant. © 2014 Wiley Periodicals, Inc.

DOI: 10.1002/qua.24685

Introduction

A lot of photonic technologies (frequency doublers, space communications, biomedical imaging) rely on the nonlinear optical (NLO) properties of matter and thereof of their constitutive units.[1] Among these, organic molecules present advantages due to their short response times and the ability of synthesis to tune their properties by proper structural modifications and functionalizations.[2] The design of efficient organic NLO compounds results from a multidisciplinary approach combining synthesis of molecules, their physicochemical characterizations, and theoretical calculations. The latter are used (i) to investigate, prior the synthesis of the relevant ones, a large set of compounds to pinpoint those with the largest responses, (ii) to deduce structure–property relationships, and (iii) also to interpret experimental data. However, after four decades of investigations, predicting the NLO properties of molecules and matter remains a challenging task for quantum chemistry, owing to the many subtle issues that need to be considered.[3] So, hierarchies of approximations as well as of interpretation schemes have been developed, considering different aspects of the prediction of NLO responses, encompassing the electron correlation effects, the vibrational contributions, the effects of the surrounding, and their frequency dispersion.[1b,4] In this contribution, two aspects related to evaluating the molecular NLO properties are tackled, the numerical differentiations of the finite field (FF) procedure and the frequency dispersion. This article is organized as follows: the next four sections introduce the definitions and the context of the FF scheme and the frequency dispersion. Then, a section is devoted to the computational details before the results are presented and discussed.

Definitions

The hyperpolarizabilities are generally defined by considering the effects of an external electric ($\vec{F}$) (electromagnetic in the most general case) field on the molecular dipole moment:

$$\vec{\mu}(\vec{F})=\vec{\mu}(0)+\overleftrightarrow{\alpha}\cdot\vec{F}+\frac{1}{2}\overrightarrow{\overleftrightarrow{\beta}}:\vec{F}\vec{F}+\ldots \quad (1)$$

or on the energy

$$E(\vec{F})=E(0)-\vec{\mu}(0)\cdot\vec{F}-\frac{1}{2!}\overleftrightarrow{\alpha}:\vec{F}\vec{F}-\frac{1}{3!}\overrightarrow{\overleftrightarrow{\beta}}:\vec{F}\vec{F}\vec{F}-\ldots \quad (2)$$

where $\vec{\mu}(0)$ is the permanent dipole moment, $\overleftrightarrow{\alpha}$ the polarizability tensor, and $\overrightarrow{\overleftrightarrow{\beta}}$ the first hyperpolarizability tensor. $E(0)$ is the zero-field energy. The different tensor components can, therefore, be determined as derivatives of the dipole moment or of the energy with respect to the external field. For instance,

$$\beta_{ijk}=-\left(\frac{\partial^3 E}{\partial F_i\partial F_j\partial F_k}\right)_0=\left(\frac{\partial^2\mu_i}{\partial F_j\partial F_k}\right)_0 \quad (3)$$

where i, j, and k refer to the applied external field directions, that is, x, y, or z.

M. de Wergifosse, V. Liégeois, Benoît Champagne
Laboratoire de Chimie Théorique, Unité de Chimie Physique Théorique et Structurale, Université de Namur, Rue de Bruxelles, 61, B-5000 Namur, Belgium
E-mail: benoit.champagne@unamur.be

Contract grant sponsor: FNRS-FRFC (Conventions Nos. 2.4.617.07.F and 2.5020.11).

The FF Method

Among the different computational schemes, the FF method[5] is an easy applicable technique, which consists of calculating the energy (or lower-order properties) for different amplitudes of the external field. It is usually based on Eq. (2), which makes it applicable to a large range of levels of approximation,[6] provided field-dependent energies can be calculated. Indeed, it only needs an extra electric field term in the Hamiltonian. By design, this method is, however, limited to static properties or rather to derivatives with respect to static electric field. Besides, an automatic application of the FF method is not obvious. In particular, the selection of an appropriate window of electric field amplitudes is a crucial parameter to achieve high accuracy and this gets more and more stringent when going toward higher and higher-order derivatives.[7] Reference [7] has established a range of feasible field strengths that guarantee reliable numerical results. Indeed, owing to the finite difference expressions to calculate the successive derivatives, the results contain contaminations from higher-order hyperpolarizabilities. These can be eliminated using the Richardson extrapolation procedure,[8] also known as Romberg differentiation in the quantum chemistry community. On the basis of calculations performed for different sets of electric field amplitudes, a Romberg table or triangle is written and can help monitoring the convergence of the numerical differentiations. Still, the analysis of the Romberg triangle is not straightforward and requires understanding the physical phenomena underlying the application of external fields to chemical compounds. Hereafter, a systematic and automatic procedure is proposed. It provides the targeted values as well as information about the convergence of the Romberg procedure. The assessment of the method is carried out at the Hartree–Fock level of calculation in comparison to benchmark analytical derivatives, which are obtained using the coupled-perturbed Hartree-Fock (CPHF) scheme.[9] Further illustrations are performed at a correlated level, using the coupled-cluster singles and doubles (CCSD) method. In that case, the numerical derivatives are estimated from orbital-relaxed field-dependent energies as well as orbital-unrelaxed field-dependent energies. Then, comparisons are made with respect to analytical derivatives obtained with the CCSD quadratic response theory (CCSD-QRF).[10]

Frequency Dispersion

The evolution of the molecular hyperpolarizabilities as a function of the frequency of the incident light is another aspect to control in order to develop efficient devices or to interpret experimental data. Besides the resonance effects that can strongly impact the NLO responses and hamper the analysis of the intrinsic responses,[11] off-resonance frequency dispersions are usually large in the UV/visible domain for π-conjugated organic molecules and deserve to be accounted for. A strongly correlated method is often desirable but time-dependent calculations are, however, not always allowed or they are too time demanding. To alleviate this issue, approximate schemes have been elaborated. They combine static hyperpolarizabilities calculated at a highly correlated level with frequency dispersion estimated at a lower one, typically by using the time-dependent Hartree-Fock (TDHF) method.[12] Sekino and Bartlett[13–15] proposed the multiplicative scheme, also previously known as percentage correction, which for β reads

$$\begin{aligned}\beta_{\text{correlated}}(-\omega_\sigma;\omega_A,\omega_B) &\approx \beta_{\text{TDHF}}(-\omega_\sigma;\omega_A,\omega_B)\frac{\beta_{\text{correlated}}(0;0,0)}{\beta_{\text{CPHF}}(0;0,0)}\\ &=\beta_{\text{correlated}}(0;0,0)\frac{\beta_{\text{TDHF}}(-\omega_\sigma;\omega_A,\omega_B)}{\beta_{\text{CPHF}}(0;0,0)}\end{aligned} \tag{4}$$

where frequency-dependent TDHF estimates are corrected by the ratio between the correlated and Hartree–Fock static response or, equivalently, where the static correlated response is corrected for the ratio between the dynamic and static Hartree–Fock values. Besides, Rice and Handy[16,17] have proposed an additive scheme where any tensor component of β is approximated by:

$$\begin{aligned}\beta_{\text{correlated}}(-\omega_\sigma;\omega_A,\omega_B) &\approx \beta_{\text{correlated}}(0;0,0)\\ &+\{\beta_{\text{TDHF}}(-\omega_\sigma;\omega_A,\omega_B)-\beta_{\text{CPHF}}(0;0,0)\}\\ =\beta_{\text{TDHF}}(-\omega_\sigma;\omega_A,\omega_B)&+\{\beta_{\text{correlated}}(0;0,0)-\beta_{\text{CPHF}}(0;0,0)\}\end{aligned} \tag{5}$$

The validity of these expressions has been assessed in a few papers, in particular with respect to the range of frequencies where it is valid. Dalskov et al.[18] concluded that whenever the approximate TDHF frequency dependence is reliable both the multiplicative and the additive schemes work quite well. Pluta and Sadlej[19] stated that the range of frequencies for which the scaling can be used should not exceed about half of the lowest computed first excitation energy. For push-pull π-conjugated systems, one of us has observed that the multiplicative scheme is superior to the additive one.[20] Using the quasienergy derivative approach at the Møller–Plesset second-order level of approximation, Aiga and Itoh[21] calculated the frequency-dependent polarizabilities and hyperpolarizabilities of H_2O and NH_3 and found a good agreement with those of Sekino and Bartlett[14] obtained using the multiplicative scheme. In this Chapter, further assessment of both approximate schemes is carried out for two π-conjugated systems where the correlated dynamic values are evaluated at the CCSD-QRF level of approximation.[10]

Kleinman's Symmetry

Kleinman symmetry is defined as the interexchangeability of all the indices in the (hyper)polarizability tensor of a system.[22] Considering the second harmonic generation (SHG) β response, the last two frequencies are identical and, therefore, the β tensor components are invariant on permuting the corresponding last two indices, $\beta_{ijk}(-2\omega;\omega,\omega)=\beta_{ikj}(-2\omega;\omega,\omega)$. Conversely, the following equality

$$\beta_{ijk}(-2\omega;\omega,\omega)=\beta_{kij}(-2\omega;\omega,\omega)=\beta_{jki}(-2\omega;\omega,\omega) \tag{6}$$

is only enforced by symmetry in the static limit or when the Kleinman symmetry is satisfied. In fact, it should be pointed

out that those conditions are satisfied for a limited range of frequencies. Nevertheless, they are routinely used to simplify the analysis of NLO measurements because they enable to reduce the number of independent components of the hyperpolarizability tensor. In certain circumstances, assuming Kleinman symmetry leads to errors, as pointed out in Ref. [23]. They used the Kramers–Kronig dispersion relations to demonstrate that the frequency window where Kleinman's symmetry is satisfied is narrower than usually admitted for a fluorescein chromophore. They showed that the Kramers–Kronig dispersion and Kleinman's relations are mutually exclusive. In this article, using CCSD-QRF β responses, the range of validity of Kleinman's symmetry conditions is further assessed by calculating the frequency dispersion of the first hyperpolarizability of π-conjugated molecules.

Molecular Structures and Computational Procedure

Two molecules were selected to tackle these frequency dispersion and numerical derivative issues, that is, (i) *p*-nitroaniline (**1**) and (ii) a derivative of the *p*-quinodimethane where the $CH_2^{(\bullet)}$ terminal units are formally replaced by one $NH_2^{(+\bullet)}$ and one $BH_2^{(-\bullet)}$[24] (**2**) groups (Fig. 1). Their geometries were optimized at the density functional theory level with the B3LYP exchange-correlation functional and the 6-311G(d) basis set. Although the hyperpolarizabilities depend on the geometries, it is not expected that changing the geometries will modify the conclusions of these investigations.

Compounds **1** and **2** belong to the C_s and C_{2v} point group, respectively. Note that the two hydrogen atoms of the NH_2 group of *p*-nitroaniline are slightly out-of-plane with respect to the rest of the molecule, implying C_s symmetry. For the C_s point group, there are 10 nonzero independent components in the SHG β tensor: β_{xxx}, β_{yyy}, β_{xxy}, β_{xyy}, β_{xzz}, β_{yzz}, β_{yxx}, β_{yyx}, β_{zzx}, and β_{zzy}. In the static limit or more generally when the Kleinman conditions are satisfied: $\beta_{xxy}=\beta_{yxx}$, $\beta_{xyy}=\beta_{yyx}$, $\beta_{xzz}=\beta_{zzx}$, and $\beta_{yzz}=\beta_{zzy}$ which reduce to six the number of independent β tensor components. For the C_{2v} point group, there are five nonzero independent components: β_{zzz}, β_{zyy}, β_{zxx}, β_{yyz}, and β_{xxz}. Again, in the static limit, some pairs of components are identical: $\beta_{zyy}=\beta_{yyz}$ and $\beta_{zxx}=\beta_{xxz}$.

The FF calculations were performed (i) at the Hartree–Fock level of approximation with the aug-cc-pVTZ basis set and (ii) at the coupled-cluster level of theory with single and double excitations for relaxed orbitals (the external electric field is added directly to the HF Hamiltonian) and nonrelaxed ones (the external electric field is added to the CCSD Hamiltonian) with the 6-31+G(d) basis set. The energies were converged to a precision of 10^{-11} a.u. The field amplitudes range from 0.0002 to 0.0064 a.u. in a geometric progression with a common ratio of $a=2$, $a=\sqrt{2}$, and $a=\sqrt[4]{2}$. To assess the accuracy of the FF calculations, the numerical values are compared to the analytical ones obtained (i) with the Coupled-Perturbed Hartree–Fock method[9] with a convergence threshold of 10^{-8} and (ii) with the CCSD-QRF method,[11] when the numerical values are obtained without orbital relaxation.

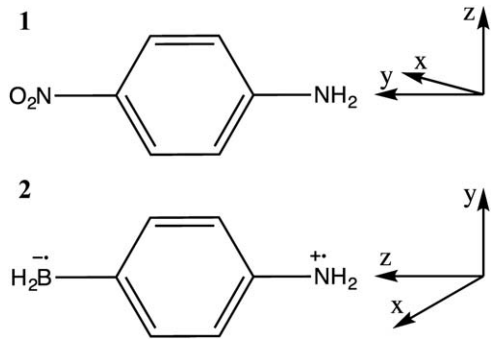

Figure 1. Structures of compounds **1** and **2** in the frame of Cartesian axes.

TDHF and CCSD-QRF calculations of β at wavelengths of 632, 713, 794, 929, 1064, 1500, and 1900 nm were carried out to assess the additive and multiplicative approximations. In addition to the tensor components, the analysis also addresses quantities that can be extracted from hyper-Rayleigh scattering (HRS) experiments, that is, β_{HRS} and the depolarization ratios.[2] Full expressions for these quantities without assuming Kleinman's conditions can be found in Ref. [25].

All reported β values are given in a.u. (1 a.u. of $\beta = 3.6213 \times 10^{-42}\ m^4\ V^{-1} = 3.2064 \times 10^{-53}\ C^3\ m^3\ J^{-2} = 8.639 \times 10^{-33}$ esu)[26] within the T convention. HF and TDHF/CPHF calculations were carried out with the Gaussian09 packages.[27] CCSD FF and QRF calculations were performed with the Dalton2011 program.[28]

Toward an Automatic Romberg Differentiation Procedure

Theory

The Romberg differentiation procedure consists in combining energy values obtained for a succession of *k* external electric fields, of which the amplitudes form a geometric progression given by $F(k)=a^kF_0$, where F_0 is the smallest field value ($F_0 = 0.0002$ a.u.) and *a* the common ratio. For the different types of β tensor components, the finite difference expressions[5,6] corresponding to the zero-order iteration read:

$$\beta_{iii}(k,0)=3\frac{[E(F_{-i}(k+1))-E(F_i(k+1))]-a[E(F_{-i}(k))-E(F_i(k))]}{a(a^2-1)(a^kF_0)^3} \tag{7}$$

$$\beta_{ijj}(k,0)=\frac{\begin{pmatrix}[E(F_{-i-j}(k))-E(F_{ij}(k))]+[E(F_{-ij}(k))-E(F_{i-j}(k))]\\-2[E(F_{-i}(k))-E(F_i(k))]\end{pmatrix}}{2(a^kF_0)^3} \tag{8}$$

$$\beta_{ijm}(k,0)=\frac{\begin{pmatrix}[E(F_{-i-j-m}(k))-E(F_{ijm}(k))]-[E(F_{-i-j}(k))-E(F_{ij}(k))]\\-[E(F_{-i-m}(k))-E(F_{im}(k))]-[E(F_{-j-m}(k))-E(F_{jm}(k))]\\+[E(F_{-i}(k))-E(F_i(k))]+[E(F_{-j}(k))-E(F_j(k))]\\+[E(F_{-m}(k))-E(F_m(k))]\end{pmatrix}}{2(a^kF_0)^3} \tag{9}$$

where the $\pm i$, $\pm j$, and $\pm m$ field indexes refer to the field directions, that is, $\pm x$, $\pm y$, or $\pm z$. These expressions are easily

obtained by combining Taylor expansions of the energy [Eq. (2)] with different amplitudes and/or directions of the external fields. These expressions are then truncated to third order. For example, to obtain Eq. (8), the corresponding Eq. (2) reads:

$$E(F_{ij}(k))=E_0-\left[\mu_i F_i(k)+\mu_j F_j(k)\right]-\frac{1}{2}\left[\alpha_{ii}F_i(k)^2+2\alpha_{ij}F_i(k)F_j(k)+\alpha_{jj}F_j(k)^2\right]-\frac{1}{3!}\left[\beta_{iii}F_i(k)^3+3\beta_{iij}F_i(k)^2F_j(k)+3\beta_{ijj}F_i(k)F_j(k)^2+\beta_{jjj}F_j(k)^3\right]-\ldots \quad (10)$$

and the following field amplitudes are used: $(F_i(k),F_j(k))=(a^kF_0,a^kF_0)$, $(-a^kF_0,-a^kF_0)$, $(-a^kF_0,a^kF_0)$, $(a^kF_0,-a^kF_0)$, $(a^kF_0,0)$, and $(-a^kF_0,0)$. Because the field amplitudes are finite, these expressions provide approximations to the true static β tensor components, and they contain contamination from higher-order hyperpolarizabilities. Equation (9) has been designed to use only two additional field amplitudes/directions $F_{ijm}(k)$ and F_{-i-j-m} (k) in addition to those already used for the previous types of components. An alternative and more accurate expression with improved higher-order hyperpolarizability cancelations to get the β_{ijm} tensor components reads:

$$\beta_{ijm}(k,0)=\frac{\left(\begin{array}{c}\left[E(F_{-i-j-m}(k))-E(F_{ijm}(k))\right]+\left[E(F_{ij-m}(k))-E(F_{-i-jm}(k))\right]\\+\left[E(F_{i-jm}(k))-E(F_{-ij-m}(k))\right]+\left[E(F_{-ijm}(k))-E(F_{i-j-m}(k))\right]\end{array}\right)}{8(a^kF_0)^3} \quad (11)$$

However, this expression requires evaluating the energy at six additional fields. To remove the contaminations from higher-order hyperpolarizabilities, successive "Romberg iterations" are carried out using a recursive expression[7,8]:

$$\beta(k,n)=\frac{a^{2n}\beta(k,n-1)-\beta(k+1,n-1)}{a^{2n}-1} \quad (12)$$

which leads to the so-called "Romberg triangle" where the convergence of the numerical derivative can be monitored. Because these expressions are based on molecular energies, their physicochemical nature can impact the convergence of the "Romberg procedure." As mentioned in Ref. [7], for any molecule there exists a field window where the finite differentiation is stable. Upper and lower bounds define this window. Field strengths below that window suffer from a too large round-off error between energy values, which is proportional to the energy convergence threshold. On the other side, the upper bound is imposed by the critical field amplitude corresponding to the intersection between the ground and excited state energies. The latter field depends on the molecule. In the Romberg differentiation procedure, this stability window defines a subtriangle, which is the "holy grail" for the analysis of the "Romberg triangle." Up to now, this analysis has mostly been carried out by "hand." However, by considering some criteria derived from the observations made in Ref. [7], a window of ideal field strengths can be automatically selected, leading to an automatic Romberg differentiation procedure.

The procedure used here is based on the analysis of field amplitude errors. The field amplitude error is defined as the difference between β values obtained for consecutive field amplitudes at the same "Romberg iteration":

$$\varepsilon_k(n)=\beta(k+1,n)-\beta(k,n) \quad (13)$$

The field error obeys to the same recursive expression as the "Romberg procedure." Thus, by the use of the recursive expression, the amplitude of the field errors along the iterations is expected to decrease. Another useful quantity is the iteration (order) error, defined as:

$$\varepsilon_n(k)=\beta(k,n+1)-\beta(k,n) \quad (14)$$

It can be seen as a quantity probing the convergence of the "Romberg procedure" between successive iterations.

The analysis starts by considering the $\beta(k,0)$ values at the iteration $n=0$. If one of the $\varepsilon_k(0)$ absolute values is smaller than a chosen threshold (10^{-2} or 10^{-3} a.u. for the first hyperpolarizability), the final β value is directly obtained and the procedure is stopped. For larger values of $\varepsilon_k(0)$, the procedure selects the set of consecutive β values for which the finite differentiation is stable. This stability region is defined by field errors of the same sign (of which the magnitude increases with the field amplitude). If there is more than one stability set, the largest set is selected, and then the set with the smallest field error. Note that, for small field amplitudes, a change of sign of the field error is often an indication that, below that field amplitude, round-off errors are present and get larger. Conversely, if all consecutive field error values have alternating signs, the smallest field error is picked up. Then, the final β value is obtained at the next iteration and the accuracy is given by the corresponding iteration error. If the last condition is not met, that is, if there exists a stability region, a selected set of values is used to go to the next iteration.

If there is no reduction of the field errors between two consecutive iterations via the recursive expression, convergence is achieved and the lowest field error from the previous iteration is selected to determine the final β value. In the other case, the "Romberg procedure" reduces the amplitude of the field errors (this corresponds to removing the high-order contaminations), and the iterative procedure is pursued until convergence.

Applications

Using the automatic method described above for field amplitudes ranging from 0.0002 to 0.0064 and $a=2$, $a=\sqrt{2}$, and $a=\sqrt[4]{2}$, the best HF/aug-cc-pVTZ β tensor components are listed in Table 1, as well as, the final iteration error and the CPHF reference results. For the dominant β_{yyy} component, the "Romberg triangles" obtained with $a=2$, $a=\sqrt{2}$, and $a=\sqrt[4]{2}$ are presented in Tables (2–4), respectively. For example, a value of -993.83 a.u. is calculated for the β_{yyy} component of compound **1** when $a=2$. At the $n=0$ iteration, the selected set of field errors goes from $k=1$ to 3. Going to the next iteration, the field error signs alternate and the smallest field error corresponds to $k=2$. The final β_{yyy} value is, therefore, obtained at iteration $n=2$ for $k=2$. For a step size of $a=\sqrt[4]{2}$

Table 1. HF/aug-cc-pVTZ β components (in a.u.) as obtained within the FF and CPHF approach for compounds **1** and **2**.

	1				2			
HF/aug-cc-pVTZ	$a=\sqrt[4]{2}$	$a=\sqrt{2}$	$a=2$	CPHF	$a=\sqrt[4]{2}$	$a=\sqrt{2}$	$a=2$	CPHF
β_{xxx}	**−3.95**	**−3.94**	**−3.94**	**−3.94**	**0.00**	**0.00**	**0.00**	**0.00**
	0.01	0.04	0.02					
β_{yyy}	**−993.82**	**−993.83**	**−993.83**	**−993.81**	**0.00**	**0.00**	**0.00**	**0.00**
	0.01	0.01	0.00					
β_{zzz}	**0.00**	**0.00**	**0.00**	**0.00**	**−1282.82**	**−1282.83**	**−1282.81**	**−1282.82**
					0.01	0.00	0.00	
β_{xyy}	**−8.79**	**−8.80**	**−8.80**	**−8.80**	**0.00**	**0.00**	**0.00**	**0.00**
	0.00	0.00	0.00					
β_{xzz}	**−3.26**	**−3.26**	**−3.26**	**−3.26**	**0.00**	**0.00**	**0.00**	**0.00**
	0.00	0.00	0.00					
β_{yzz}	**176.41**	**176.40**	**176.40**	**176.41**	**0.00**	**0.00**	**0.00**	**0.00**
	0.00	0.00	0.00					
β_{xxy}	**36.03**	**36.01**	**35.99**	**36.01**	**0.00**	**0.00**	**0.00**	**0.00**
	0.01	0.00	0.00					
β_{xxz}	**0.00**	**0.00**	**0.00**	**0.00**	**−53.38**	**−53.36**	**−53.36**	**−53.37**
					0.00	0.00	0.00	
β_{yyz}	**0.00**	**0.00**	**0.00**	**0.00**	**65.41**	**65.41**	**65.41**	**65.41**
					0.00	0.00	0.00	
β_{xyz}	**0.00**	**0.00**	**0.01**	**0.00**	**0.00**	**0.00**	**0.01**	**0.00**
	0.00	0.00	0.00		0.00	0.00	0.00	
β_{HRS}	**387.16**	**387.17**	**387.17**	**387.16**	**530.85**	**530.85**	**530.85**	**530.85**
DR	**3.22**	**3.22**	**3.22**	**3.22**	**4.86**	**4.86**	**4.86**	**4.86**

The reported FF values were determined from analyzing the Romberg table obtained for calculations performed with field amplitudes ranging from 0.0002 to 0.0064 a.u. and common ratios $a=2$, $a=\sqrt{2}$, and $a=\sqrt[4]{2}$. The corresponding absolute values of the final iteration error are also given.

(Table 4) (i) at $n=0$, the region of stability of the field errors goes from $k=8$ to 18, (ii) going to $n=1$, the set is restricted to the $k=15$–17 region, and finally (iii) $n=2$, there is no reduction of the field errors with respect to the previous iteration and the final value corresponds to $n=2$ and $k=16$.

Using $a=2$, the FF calculations are in a good agreement with the CPHF results with less than 0.06% of difference for any nonzero component. For $a=2$, the algorithm selects the value for $n=2$ and $k=2$ and a final estimate of −993.83 a.u., which differs by 2×10^{-3}% from the CPHF value. For $a=\sqrt{2}$ (Table 3) and $a=\sqrt[4]{2}$ (Table 4) many field amplitudes are used, 11 and 21, respectively. Therefore, at $n=0$, the selected stability zone is larger but, upon iteration, it rapidly shrinks to define the final estimates, which are similar to that with $a=2$. In view of comparison with experiment, the value of interest is β_{HRS} and Table 1 shows that the same value is obtained using the three common ratios.

For the determination of the β_{zzz} component of molecule **2**, the analysis of the "Romberg table" is presented in Supporting Information Tables S1–S3 for step sizes of $a=2$, $a=\sqrt{2}$, and $a=\sqrt[4]{2}$, respectively. As for molecule **1**, the external field window is sufficiently large to include the stability area where the field differentiations are stable. In the case of $a=2$, the algorithm selects a final value of −1282.81 a.u. for $k=2$ and $n=2$. The difference with respect to the CPHF value is again negligible. Using $a=\sqrt{2}$ gives a converged value for $k=5$ at iteration $n=4$. A similar result is obtained for $a=\sqrt[4]{2}$. Similar analyses can be made for the other tensor components and, therefore, for the β_{HRS} quantity. Note that (i) the numerical approach is also able to predict the zero values for those components, which are zero by symmetry and that (ii) such a numerical accuracy on β_{HRS} is largely superior to the precision achieved nowadays experimentally.

In the following, $a=2$ is used for CCSD calculations because it requires less field-dependent energy calculations. Indeed,

Table 2. "Romberg triangle" for the determination of β_{yyy} of compound **1** at the HF/aug-cc-pVTZ level with a step size $a=2$. [Color table can be viewed in the online issue, which is available at wileyonlinelibrary.com.]

	$n=0$		$n=1$		$n=2$		$n=3$		$n=4$
$k=0$	−993.69	−0.02	−993.71	−0.02	−993.73	−0.01	−993.73	0.00	−993.73
	0.05		0.32		0.37		0.38		
$k=1$	−993.64	0.26	−993.39	0.03	−993.36	0.01	−993.35		
	−0.77		−0.45		−0.48				
$k=2$	−994.41	0.58	−993.83	**−0.00**	**−993.83**				
	−1.73		**0.02**						
$k=3$	−996.14	2.33	−993.81						
	−7.0								
$k=4$	−1003.13								

The field amplitude errors and the iteration order errors are written in blue (between the lines) and in red (between the columns), respectively. The final field amplitude and iteration errors are underlined and in bold. The final β_{yyy} is in bold.

Table 3. Part of the "Romberg triangle" for the determination of β_{yyy} of compound **1** at the HF/aug-cc-pVTZ level with a step size $a=\sqrt{2}$. [Color table can be viewed in the online issue, which is available at wileyonlinelibrary.com.]

	$n=0$		$n=1$		$n=2$		$n=3$		$n=4$
$k=4$	−994.05	0.41	−993.64	0.01	−993.63	0.00	−993.63	0.00	−993.63
	−0.41		−0.04		0.01		0.05		0.07
$k=5$	−994.46	0.78	−993.68	0.06	−993.62	−0.04	−993.58	−0.02	−993.56
	−0.78		−0.20		−0.28		−0.34		
$k=6$	−995.24	1.36	−993.88	−0.02	−993.90	−0.01	−993.91		
	−1.37		0.06		0.07				
$k=7$	−996.61	2.79	−993.82	**−0.01**	**−993.83**				
	−2.78		**0.03**						
$k=8$	−999.39	5.60	−993.79						
	−5.61								
$k=9$	−1005.00								

The field amplitude errors and the iteration order errors are written in blue (between the lines) and in red (between the columns), respectively. The final field amplitude and iteration errors are underlined and in bold. The final β_{yyy} is in bold.

the number of calculations needed to obtain the whole first hyperpolarizability tensor for field amplitudes going from 0.0002 to 0.0064 with $a=2$, $a=\sqrt{2}$, and $a=\sqrt[4]{2}$ are, respectively, 120, 220, and 420. With the availability of today's computer architectures, these large numbers of calculations can be run simultaneously, leading to effectiveness comparable to a massively parallel calculation. In these calculations, an *a priori* large field amplitudes window is used to be certain to encompass the stable subwindow. Then, using the automatic Romberg differentiation procedure, the range of field amplitudes is narrowed. For instance, for β_{yyy} with $a=2$, the stable subwindow is defined by field amplitudes ranging from 0.0008 to 0.0064 a.u., at the HF level of calculation. It is, therefore, chosen for the calculations at the correlated level of theory, to decrease the number of calculations.

We now consider the CCSD first hyperpolarizability calculations. Table 5 compares the FF and CCSD-QRF results. For the *p*-nitroaniline, in both relaxed/nonrelaxed CCSD calculations, all the components of the first hyperpolarizability tensor converge rapidly with a final iteration order error of ±0.02 a.u. or less (Tables 6 and 7). As expected, the nonrelaxed CCSD FF results and the QRF ones are basically identical. The relaxed CCSD results are slightly smaller than the unrelaxed ones, leading to β_{HRS} (relaxed) of 679 a.u. and β_{HRS} (nonrelaxed) of 739 a.u. Comparisons between the nonrelaxed and relaxed orbitals approaches in coupled cluster calculations were already debated in 1987 by Salter et al.,[29] who demonstrated numerically and proved formally that the CCSD model using nonrelaxed orbitals is able to include most of the relaxation effects for the evaluation of first- and second-order properties but some small differences are observed for higher-order properties like the first hyperpolarizability. In the case of first hyperpolarizability, they showed for the HF molecule that the response is 3.2% higher for the nonrelaxed orbitals with respect to the relaxed ones. They speculated that this difference could originate from different numerical precisions. Later, O'Neil et al.[30] pointed out that including orbital relaxation in the reference determinant introduces an extra set of unphysical poles in the CC response, which leads in the case of static electrical properties to results not necessarily more precise. For compound **2**, similar conclusions can be drawn. In Supporting Information Table S4, it is shown that the nonrelaxed CCSD β_{zzz} component converges rapidly. However, in the relaxed case, the "Romberg triangle" is less stable and it might benefit from the use of a smaller step size and/or a smaller energy threshold (Supporting Information Table S5).

For determining the CCSD β_{xyz} of compounds **1** and **2**, which, by symmetry, should be equal to zero, Eq. (11) was preferentially used. It shows for both compounds a better stability and leads to

Table 4. Part of the "Romberg triangle" for the determination of β_{yyy} of compound **1** at the HF/aug-cc-pVTZ level with a step size $a=\sqrt[4]{2}$. [Color table can be viewed in the online issue, which is available at wileyonlinelibrary.com.]

	$n=0$		$n=1$		$n=2$		$n=3$		$n=4$
$k=14$	−996.05	2.26	−993.79	0.03	−993.76	0.04	−993.72	0.04	−993.68
	−0.94		−0.03		−0.08		−0.13		−0.18
$k=15$	−996.99	3.17	−993.82	−0.02	−993.84	−0.01	−993.85	0.01	−993.86
	−1.31		0.01		0.02		0.04		
$k=16$	−998.30	4.49	−993.81	**−0.01**	**−993.82**	0.01	−993.81		
	−1.86		**0.01**		−0.02				
$k=17$	−1000.17	6.37	−993.80	−0.04	−993.84				
	−2.64		0.04						
$k=18$	−1002.81	9.05	−993.76						
	−3.75								
$k=19$	−1006.56								

The field amplitude errors and the iteration order errors are written in blue (between the lines) and in red (between the columns), respectively. The final field amplitude and iteration errors are underlined and in bold. The final β_{yyy} is in bold.

Table 5. CCSD/6–31+G(d) β components (in a.u.) as obtained within the FF and QRF approaches for compounds **1** and **2.**

	1			2		
CCSD 6–31+G(d)	Relaxed orbitals	Nonrelaxed orbitals	Quadratic response functions	Relaxed orbitals	Nonrelaxed orbitals	Quadratic response functions
β_{xxx}	**−16.23**	**−17.97**	**−17.92**	**0.01**	**0.00**	**0.00**
	0.02	0.00		0.00		
β_{yyy}	**−1699.26**	**−1848.00**	**−1848.32**	**−0.04**	**0.00**	**0.00**
	0.00	0.02		0.01		
β_{zzz}	**0.01**	**0.00**	**0.00**	**−2387.99**	**−2628.69**	**−2628.35**
	0.00	0.00		0.31	0.02	
β_{xyy}	**−20.36**	**−25.14**	**−25.13**	**0.00**	**0.00**	**0.00**
	0.00	0.00				
β_{xzz}	**−3.26**	**−3.31**	**−3.31**	**0.00**	**0.00**	**0.00**
	0.00	0.02				
β_{yzz}	**105.05**	**110.58**	**110.61**	**0.00**	**0.00**	**0.00**
	0.00	0.00				
β_{xxy}	**49.61**	**52.86**	**52.32**	**0.00**	**0.00**	**0.00**
	0.00	0.00				
β_{xxz}	**0.00**	**0.00**	**0.00**	**−47.23**	**−48.33**	**−48.40**
				0.00	0.01	
β_{yyz}	**0.00**	**0.00**	**0.00**	**54.19**	**68.53**	**68.51**
				0.00	0.00	
β_{xyz}	**0.00**	**0.00**	**0.00**	**0.00**	**0.00**	**0.00**
$\beta_{HRS,\infty}$	**678.89**	**739.00**	**739.21**	**988.19**	**1085.60**	**1085.47**
DR	**4.19**	**4.21**	**4.21**	**4.96**	**4.92**	**4.92**

The reported FF values were determined from analyzing the Romberg table obtained for calculations performed with field amplitudes ranging from 0.0002 to 0.0064 a.u. and common ratios $a = 2$. The corresponding absolute values of the final iteration error are also given.

β_{xyz} values less than 0.005 a.u. Conversely, using Eq. (9), the relaxed CCSD values of compounds **1** and **2** amount to 0.03 and 0.02 a.u., whereas in the nonrelaxed case, 0.06 and −0.03 a.u., respectively. The question is of course to know whether, for large systems, this small improvement is worth because it requires additional, resource-expensive, calculations.

Approximate Frequency Dispersions of the First Hyperpolarizability from Correlated Calculations

The performance of the multiplicative and additive schemes to describe the frequency dispersion of the CCSD first hyperpolarizability is tackled in Figure 2 and Table 8 for compounds **1** and **2**, where CCSD-QRF results are used as a benchmark. At large wavelength (1900 nm), the errors made by both approximations remain smaller than 3 and 7%: the additive approximation underestimates by 5.8 and 6.1% the β_{HRS} CCSD-QRF reference value of compounds **1** and **2**, respectively, whereas within the multiplicative scheme, these drop to 2.5 and 1.9%. Then, the underestimations grow with the frequency. At 1064 nm, which is also a typical laser wavelength, the multiplicative scheme underestimates the HRS first hyperpolarizability of **1** by 9.3% and it goes up to 18.3% when using the additive scheme. Similar differences are observed for compound **2**. Going further toward smaller wavelengths, the errors increase and the additive approximation gets very poor.

An alternative way to determine the correlated dynamic first hyperpolarizabilities consists in applying the two-state approximation (TSA),[31] which assumes that only one excited state contributes to the first hyperpolarizability and that this excited state governs the frequency dispersion. In the case of SHG β,

Table 6. "Romberg triangle" for the determination of the β_{yyy} component of compound **1** at the nonrelaxed CCSD/6-31+G(d) level with a step size $a = 2$. [Color table can be viewed in the online issue, which is available at wileyonlinelibrary.com.]

	$n = 0$		$n = 1$		$n = 2$		$n = 3$		$n = 4$
$k = 0$	−1829.94	6.48	−1823.46	1.71	−1821.75	0.44	−1821.32	0.11	−1821.21
	−19.43		−25.63		−27.41		−27.86		
$k = 1$	−1849.37	0.28	−1849.09	−0.07	−1849.16	−0.02	−1849.18		
	−0.84		1.07		1.16				
$k = 2$	−1850.21	2.19	−1848.02	**0.02**	**−1848.00**				
	−6.58		**−0.22**						
$k = 3$	−1856.79	8.55	−1848.24						
	−25.63								
$k = 4$	−1882.42								

The field amplitude errors and the iteration order errors are written in blue (between the lines) and in red (between the columns), respectively. The final field amplitude and iteration errors are underlined and in bold. The final β_{yyy} is in bold.

Table 7. "Romberg triangle" for the determination of the β_{yyy} component of compound **1** at the relaxed CCSD/6-31G+(d) level with a step size $a = 2$. [Color table can be viewed in the online issue, which is available at wileyonlinelibrary.com.]

	$n=0$		$n=1$		$n=2$		$n=3$		$n=4$
$k=0$	−1722.31	−7.08	−1729.39	−1.88	−1731.27	−0.48	−1731.75	−0.12	−1731.87
	21.24		28.27		30.03		30.47		
$k=1$	−1701.07	−0.05	−1701.12	−0.12	−1701.25	−0.03	−1701.28		
	0.16		1.86		1.99				
$k=2$	−1700.91	1.65	−1699.26	**0.00**	**−1699.26**				
	−4.96		**−0.01**						
$k=3$	−1705.87	6.60	−1699.27						
	−19.81								
$k=4$	−1725.68								

The field amplitude errors and the iteration order errors are written in blue (between the lines) and in red (between the columns), respectively. The final field amplitude and iteration errors are underlined and in bold. The final β_{yyy} is in bold.

$$\beta(-2\omega;\omega,\omega) \approx \beta(0;0,0)\frac{\omega_{ge}^4}{(\omega_{ge}^2-4\omega^2)(\omega_{ge}^2-\omega^2)} \qquad (15)$$

where $\hbar\omega_{ge}=\omega_{ge}$ is the excitation energy. It can thus be employed at different levels of approximation. At the CCSD/6-31+G(d) level of theory the excitation energy of compounds **1** and **2** amounts to 4.72 and 4.58 eV and the oscillator strengths to 0.43 and 0.56, respectively. The selection of the *dominant* excited state is not always straightforward but for π-conjugated systems it is the lowest-energy excited state with large oscillator strength. In such a case, Eq. (15) provides an excellent approximation to the frequency dispersion of the first hyperpolarizability (Fig. 2). Because for large systems it is not always possible to perform excitation energy calculations at a highly correlated level, an alternative consists in evaluating these at the TDHF (usually called RPA for random phase approximation) level, which then provides a good approximation to the TDHF dispersion applied within the multiplicative scheme (Fig. 2) and underestimates the CCSD-QRF values. For compound **1** and **2**, the RPA excitation energies are 5.12 and 5.06 eV and the oscillator strengths 0.36 and 0.43, respectively.

In conclusions, describing at a high-level of theory, that is, by including electron correlation effects, the frequency dispersion of the first hyperpolarizabilities is a difficult challenge when using approximate schemes. These investigations on model π-conjugated compounds have found the following method ordering, from the less reliable to the best one: the additive scheme using TDHF dispersion, the multiplicative scheme using TDHF dispersion, TSA based on RPA excitation energies, and TSA based on CCSD excitation energies.

Deviation from Kleinman's Symmetry Conditions

The importance of deviations from the Kleinman's symmetry conditions is assessed for the SHG β response of compounds

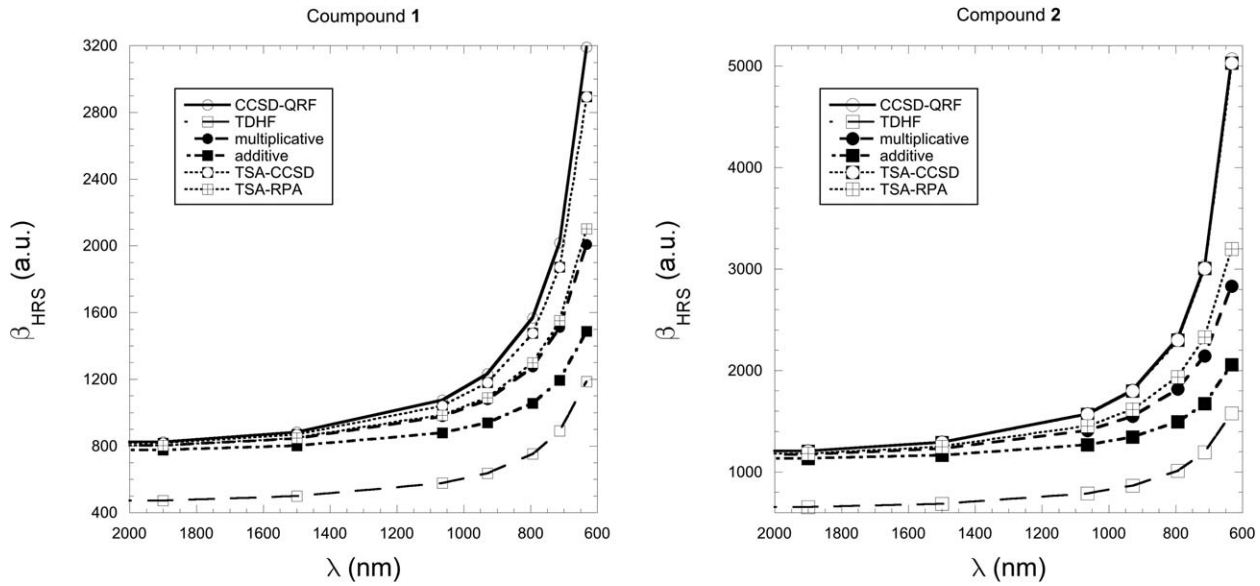

Figure 2. Frequency dispersion of β_{HRS} for compounds **1** and **2**, as calculated using the multiplicative and additive schemes from unrelaxed-orbital CCSD static values and HF frequency dispersions. Comparisons are made with respect to the reference CCSD-QRF values as well as to TDHF results and TSA dispersions. TSA-CCSD refers to Eq. (15) with excitation energies calculated at the CCSD level of theory whereas TSA-RPA when the excitation energies are calculated with the TDHF/RPA method. Lines are guides for the eyes.

Table 8. Performance of approximate schemes to describe the frequency dispersion of β_{HRS} at 1900 and 1064 nm together with the characteristics of the lowest-energy dipole-allowed excitation, evaluated at the CCSD level of approximation.

		% error on β_{HRS} (1900 nm)			% error on β_{HRS} (1064 nm)		
	ΔE (f) in eV	Additive	Multiplicative	TSA-CCSD	Additive	Multiplicative	TSA-CCSD
1	4.72 (0.43)	−6%	−3%	−1%	−18%	−9%	−3%
2	4.58 (0.56)	−6%	−3%	0%	−19%	−10%	0%

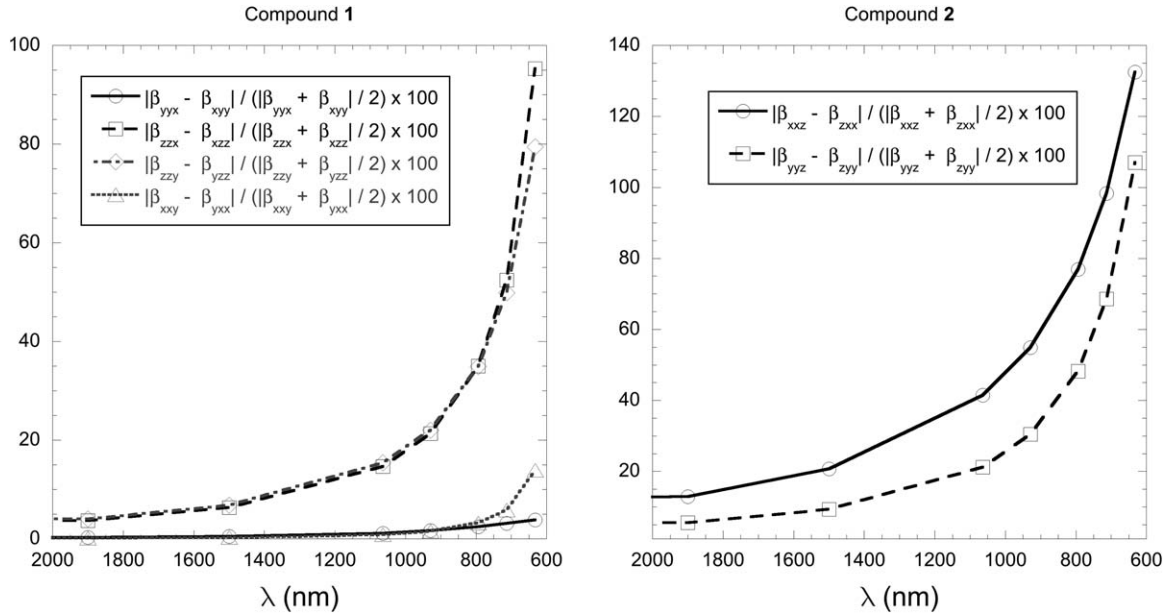

Figure 3. Deviations from Kleinman's symmetry conditions for the nonvanishing independent β tensor components of compounds **1** and **2**, as determined at the CCSD-QRF/6–31+G(d) level of theory. The lines are guides for the eyes.

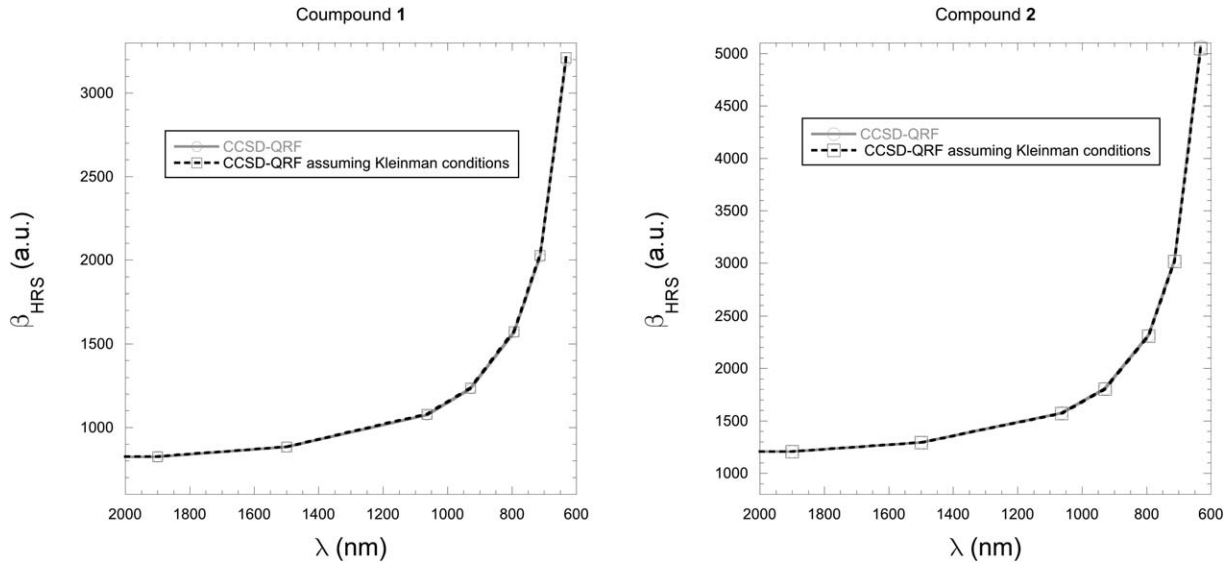

Figure 4. Frequency dispersion of β_{HRS} for compounds **1** and **2**, at the CCSD-QRF level of theory, assuming or not the Kleinman's conditions. The Kleinman's conditions have been assumed by taking the average of the two different components considered, $(\beta_{ijj}+\beta_{jii})/2=\beta_{ijj}^{eff}=\beta_{iji}^{eff}=\beta_{jii}^{eff}$, and using these in the β_{HRS} expression.

1 and **2** by analyzing the evolution of the following expression as a function of the frequency (Fig. 3):

$$(\%)_{iij\rightarrow jii} = \frac{|\beta_{iij} - \beta_{jii}|}{|\beta_{iij} + \beta_{jii}|/2} 100 \quad (16)$$

If Kleinman's conditions are satisfied, including in the static limit, the two components are identical and $(\%)_{iij \rightarrow jii}$ vanishes. For **1**, a strong deviation is observed for (β_{zzx}vs. β_{xzz}) and (β_{zzy}vs. β_{yzz}), whereas for (β_{yyx}vs. β_{xyy}) and (β_{xxy}vs. β_{yxx}) Kleinman's conditions remain valid for wavelengths as large as 1064 nm. However, the deviations amplitudes are not related to the amplitude of the β tensor components because, for example, β_{zzx} is about 17 times smaller than β_{zzy}. For the overall response, that is, β_{HRS} (see Fig. 4), assuming or not the Kleinman's condition, has negligible effects because β_{yyy} is 17 times larger than the next largest component, β_{zzy}, and its frequency dispersion is dominating the response. For compound **2**, deviations as large as 5–15% are already observed at $\lambda = 1900$ nm, precluding the use Kleinman's conditions to simplify the β analysis. As seen in Figure 4, the Kleinman's conditions impact on the β_{HRS} for compound **2**, is also negligible because β_{HRS} is at least 37 times larger than the components that are impacted by Kleinman's conditions.

Conclusions

In this article, two aspects of computing the first hyperpolarizabilities of organic compounds have been tackled, (i) the selection of a first hyperpolarizability value when using the FF procedure and (ii) the frequency dispersion of these second-order NLO responses. It has been shown that accurate numerical derivatives can be obtained by resorting to the Romberg's method and by analyzing the Romberg's table in terms of two quantities, the field error and the iteration error. This leads to selecting in Romberg's table first hyperpolarizability values, which are in close agreement with those obtained within an analytical differentiation procedure. Then, the reliability of the multiplicative and additive approximate schemes to describe the frequency dispersion at correlated levels from using HF frequency dispersion has been confirmed to be limited to large wavelengths or far-from-resonance wavelength regions. Nevertheless, the multiplicative scheme appears to be more accurate than the additive one. Besides these schemes, it was demonstrated that the key quantity is the excitation energy of the dominant excited state, which can be combined with the TSA to predict rather accurate frequency-dependent values for those systems. Finally, Kleinman's symmetry conditions are assessed, showing that for off-diagonal components, the deviations could be substantial. Nevertheless, if these off-diagonal components contributions are negligible with respect to the diagonal ones, good accuracy is achieved for experimentally related quantities like β_{HRS}.

Acknowledgments

V.L. thanks the F.R.S.-FNRS for his research associate position. The calculations were performed on the computing facilities of the Consortium des Équipements de Calcul Intensif (CÉCI), in particular those of the Plateforme Technologique de Calcul Intensif (PTCI) installed in the University of Namur.

Keywords: first hyperpolarizability · finite field · frequency dispersion · Kleinman's symmetry · Romberg quadrature

How to cite this article: M. Wergifosse, V. Liégeois, B. Champagne. *Int. J. Quantum Chem.* **2014**, *114*, 900–910. DOI: 10.1002/qua.24685

Additional Supporting Information may be found in the online version of this article.

[1] (a) H. Nalwa, S. Miyata, Nonlinear Optics of Organic Molecules and Polymers, Vol. *1*; CRC Press: Boca Raton, **1996**; (b) M. G. Papadopoulos, A. J. Sadlej, J. Leszczynski, *Non-linear Optical Properties of Matter - From Molecules to Condensed Phases*, Vol. *1*; Springer, Boca Raton, Florida, **2006**.
[2] T. Verbiest, K. Clays, V. Rodriguez, Second-Order Nonlinear Optical Characterization Techniques, 1st ed.; CRC Press, Boca Raton, Florida, **2009**.
[3] D. M. Bishop, P. Norman, In Handbook of Advanced Electronic and Photonic Materials and Devices, Vol. *9*; H. S. Nalwa, Ed.; Academic Press, Waltham, Massachusetts, **2001**.
[4] B. Champagne, B. Kirtman, In Handbook of Advanced Electronic and Photonic Materials and Devices; H. S. Nalwa, Ed.; Academic Press: San Diego, **2001**; p. 63.
[5] H. D. Cohen, C. C. J. Roothaan, *J. Chem. Phys.* **1965**, *43*, S34.
[6] (a) R. J. Bartlett, G. D. Purvis, *Phys. Rev. A* **1979**, *20*, 1313; (b) H. A. Kurtz, J. J. P. Stewart, K. M. Dieter, *J. Comput. Chem.* **1990**, *11*, 82; (c) F. Sim, S. Chin, M. Dupuis, J. E. Rice, *J. Phys. Chem.* **1993**, *97*, 1158; (d) M. Medved', M. Stachová, D. Jacquemin, J.-M. André, E. A. Perpète, *J. Mol. Struct. THEOCHEM* **2007**, *847*, 39.
[7] A. A. K. Mohammed, P. A. Limacher, B. Champagne, *J. Comput. Chem.* **2013**, *34*, 1497.
[8] L. F. Richardson, J. A. Gaunt, *Philos. Trans. R. Soc. London Ser. A* **1927**, *226*, 299.
[9] (a) T. C. Caves, M. Karplus, *J. Chem. Phys.* **1969**, *50*, 3649; (b) P. W. Langhoff, M. Karplus, R. P. Hurst, *J. Chem. Phys.* **1966**, *44*, 505.
[10] (a) C. Hättig, O. Christiansen, H. Koch, P. Jørgensen, *Chem. Phys. Lett.* **1997**, *269*, 428; (b) C. Hättig, P. Jørgensen, *Theor. Chem. Acc.* **1998**, *100*, 230.
[11] F. Mançois, J.-L. Pozzo, J. Pan, F. Adamietz, V. Rodriguez, L. Ducasse, F. Castet, A. Plaquet, B. Champagne, *Chem. Eur. J.* **2009**, *15*, 2560.
[12] (a) H. Sekino, R. J. Bartlett, *J. Chem. Phys.* **1986**, *85*, 976; (b) S. P. Karna, M. Dupuis, *J. Comput. Chem.* **1991**, *12*, 487.
[13] H. Sekino, R. J. Bartlett, *J. Chem. Phys.* **1991**, *94*, 3665.
[14] H. Sekino, R. J. Bartlett, *J. Chem. Phys.* **1993**, *98*, 3022.
[15] H. Sekino, R. J. Bartlett, *Chem. Phys. Lett.* **1995**, *234*, 87.
[16] J. E. Rice, N. C. Handy, *J. Chem. Phys.* **1991**, *94*, 4959.
[17] J. E. Rice, N. C. Handy, *Int. J. Quantum Chem.* **1992**, *43*, 91.
[18] E. K. Dalskov, H. J. A. A. Jensen, J. Oddershede, *Mol. Phys.* **1997**, *90*, 3.
[19] T. Pluta, A. J. Sadlej, *J. Chem. Phys.* **2001**, *114*, 136.
[20] D. Jacquemin, B. Champagne, C. Hättig, *Chem. Phys. Lett.* **2000**, *319*, 327.
[21] F. Aiga, R. Itoh, *Chem. Phys. Lett.* **1996**, *251*, 372.
[22] D. A. Kleinman, *Phys. Rev.* **1962**, *126*, 1977.
[23] C. A. Dailey, B. J. Burke, G. J. Simpson, *Chem. Phys. Lett.* **2004**, *390*, 8.
[24] M. de Wergifosse, F. Wautelet, B. Champagne, R. Kishi, K. Fukuda, H. Matsui, M. Nakano, *J. Phys. Chem. A* **2013**, *117*, 4709.
[25] R. Bersohn, Y.-H. Pao, H. L. Frisch, *J. Chem. Phys.* **1966**, *45*, 3184.
[26] D. P. Shelton, J. E. Rice, *Chem. Rev.* **1994**, *94*, 3.
[27] M. J. Frisch, G. W. Trucks, H. B. Schlegel, G. E. Scuseria, M. A. Robb, J. R. Cheeseman, G. Scalmani, V. Barone, B. Mennucci, G. A. Petersson, H. Nakatsuji, M. Caricato, X. Li, H. P. Hratchian, A. F. Izmaylov, J. Bloino, G. Zheng, J. L. Sonnenberg, M. Hada, M. Ehara, K. Toyota, R. Fukuda, J.

Hasegawa, M. Ishida, T. Nakajima, Y. Honda, O. Kitao, H. Nakai, T. Vreven, J. A. Montgomery, Jr., J. E. Peralta, F. Ogliaro, M. Bearpark, J. J. Heyd, E. Brothers, K. N. Kudin, V. N. Staroverov, R. Kobayashi, J. Normand, K. Raghavachari, A. Rendell, J. C. Burant, S. S. Iyengar, J. Tomasi, M. Cossi, N. Rega, J. M. Millam, M. Klene, J. E. Knox, J. B. Cross, V. Bakken, C. Adamo, J. Jaramillo, R. Gomperts, R. E. Stratmann, O. Yazyev, A. J. Austin, R. Cammi, C. Pomelli, J. W. Ochterski, R. L. Martin, K. Morokuma, V. G. Zakrzewski, G. A. Voth, P. Salvador, J. J. Dannenberg, S. Dapprich, A. D. Daniels, O. Farkas, J. B. Foresman, J. V. Ortiz, J. Cioslowski, D. J. Fox, Gaussian 09, Revision C.02; Gaussian, Inc.: Wallingford, CT, **2009**.

[28] DALTON, a molecular electronic structure program, Release Dalton 2011; **2011**. Available at: http://daltonprogram.org/. Accessed on March 2013.

[29] E. A. Salter, H. Sekino, R. J. Bartlett, *J. Chem. Phys.* **1987**, *87*, 502.

[30] D. P. O'Neill, M. Kallay, J. Gauss, *J. Chem. Phys.* **2007**, *127*, 134109.

[31] J. L. Oudar, D. S. Chemla, *J. Chem. Phys.* **1977**, *66*, 2664.

Received: 27 February 2014
Revised: 28 March 2014
Accepted: 2 April 2014
Published online 29 April 2014